

# Boronic Acid Based Modular Fluorescent Sensors for Glucose

Marcus D. Phillips<sup>1</sup> and Tony D. James<sup>1,2</sup>

Received December 12, 2003; accepted January 14, 2004

Modular photoinduced electron transfer (PET) sensors bearing two phenylboronic acid groups, one or two fluorophores: pyrene(a), phenanthrene(b), anthracene(c), 1-naphthalene(d), 2-naphthalene(e) and alkylene linkers, from trimethylene(3) to octamethylene(8), have been evaluated. Systems with a single pyrene fluorophore **3**<sub>4a</sub>, **3**<sub>5a</sub> and **3**<sub>6a</sub> bind the strongest with D-glucose (**3**<sub>6a</sub> also binds well with D-melibiose). Whilst **3**<sub>7a</sub> and **3**<sub>8a</sub> bind the strongest with D-galactose. Changing the fluorophore, also, influences the binding, **3**<sub>6a</sub>, **3**<sub>6b</sub> and **3**<sub>6c</sub> are D-glucose selective, whilst **3**<sub>6d</sub> and **3**<sub>6e</sub> are D-galactose selective. Systems with two fluorophores **3**<sub>6a-a</sub> and **3**<sub>6a-b</sub> show an overall decrease in binding efficiency. Energy transfer in **3**<sub>6a-b</sub> results in enhanced sensitivity and selectivity towards D-glucose.

**KEY WORDS:** Saccharide; glucose; recognition; sensors; fluorescence; boronic acid.

## INTRODUCTION

The chemistry of saccharides is of paramount importance to a wealth of biological functions within nature. By providing the building blocks for processes ranging from the production of metabolic energy through to tissue recognition, saccharides have found themselves to be the focus of a vast body of research aimed at understanding and mimicking their specific role and function at a cellular level [1].

Unsurprisingly the ability to derive synthetic receptors with the capacity to selectively detect specific saccharides and signal this presence by altering their optical signature has captured the attention of supramolecular chemists [2–18]. The molecular recognition of D-glucose has proved of particular interest. This single monosaccharide provides the energy for most cells of higher organisms. The breakdown of D-glucose transport within humans has been correlated to diseases such as: renal glycosuria, [19,20] cystic fibrosis [21], cancer [22] and diabetes [23,24]. Clear evidence exists that tight control of blood sugar levels in diabetics sharply reduces the

risk of the debilitating long term complications associated with this autoimmune disease [25]. Within industry applications range from the monitoring of fermenting processes to establishing the enantiomeric purity of synthetic drugs.

Current enzymatic detection methods of sugars offer specificity for only a few saccharides, additionally enzyme based sensors are unstable under harsh conditions [26]. Through synthetic design however, there exists the potential to develop stable sensors for saccharides, which could be both sensitive and selective for any chosen saccharide.

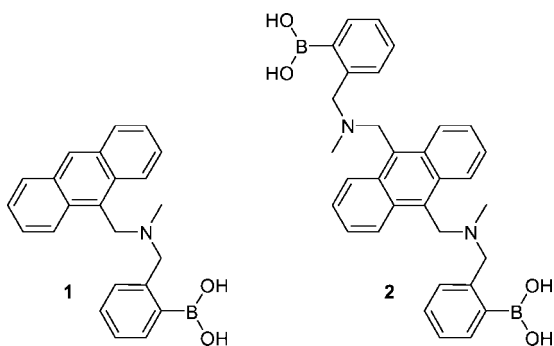
To date the vast majority of synthetic systems developed to recognise saccharides have relied upon hydrogen bonding interactions for the purposes of recognition and binding of guest species. It is the case however, that in aqueous systems neutral guests may be heavily solvated. As of yet there has been no designed, hydrogen bonding, monomeric receptor that has been able to compete effectively with bulk water for low concentrations of monosaccharide substrates. For this reason boronic acids have been studied as receptors [2,6,8,15,17,27–30]. In aqueous basic media, boronic acids are known to form, rapidly and reversibly, five- and six-membered cyclic esters with *cis*-1,2- and 1,3-diols respectively [31,32]. Due to their linked array of hydroxy groups saccharides provide an ideal structural framework for binding to boronic acids. As this interaction is covalent, it allows saccharide

<sup>1</sup> Department of Chemistry, University of Bath, Bath, BA2 7AY, United Kingdom.

<sup>2</sup> To whom correspondence should be addressed. E-mail: t.d.james@bath.ac.uk

recognition without the problem of undesired solvent-guest competition occurring at the receptor.

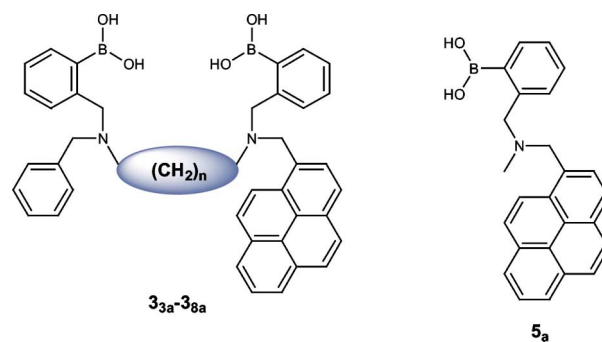
Our interest has concerned the interaction between boronic acids (Lewis acids) and neighbouring tertiary amines (Lewis bases); an interaction that provides two distinct advantages. Firstly, the interaction between the boronic acid and tertiary amine lowers the  $pK_a$  of the boronic acid, allowing molecular recognition to occur in aqueous solvents at neutral pH. Secondly, due to the contraction of the O—B—O bond angle on complexation, the Lewis acidity of the boronic acid is increased further still upon saccharide binding [33]. This reduction in  $pK_a$  is the basis of many of the sensors developed as the change is sufficient to modulate photoinduced electron transfer (PET) between the tertiary amine and an appended fluorophore [6]. This characteristic allows a fluorescent “off-on” response to be produced by boronic acid-tertiary amine based sensory systems.



The first rationally designed fluorescent PET sensor for saccharides utilising the boronic acid-tertiary amine interaction was documented in 1994 [34,35]. The monoboronic acid system displayed the same trend in selectivity towards saccharides as reported by Lorand and Edwards, indeed it follows a selectivity order, which appears to be inherent to all monoboronic acids (D-fructose > D-galactose > D-glucose) [32].

The monoboronic acid based sensor **1** was improved with the introduction of a second boronic acid group [35,36]. In this instance, saccharide binding needs to occur at both boronic acid groups to result in fluorescence enhancement. This allows two possible binding modes to arise with the formation of either a 2:1 complex or a 1:1 complex. The enhanced binding constant derived from the formation a cyclic 1:1 complex and the fortuitous spacing of the boronic acid groups meant that the diboronic acid sensor **2** was selective for D-glucose over other monosaccharides.

Whilst sensors developed around the anthracene core unit provided selectivity for sugars such as D-glucose and D-glucosamine hydrochloride [37], the anthracene core unit, acting as both the core and fluorophore limited further development of the system. It was deemed important to use

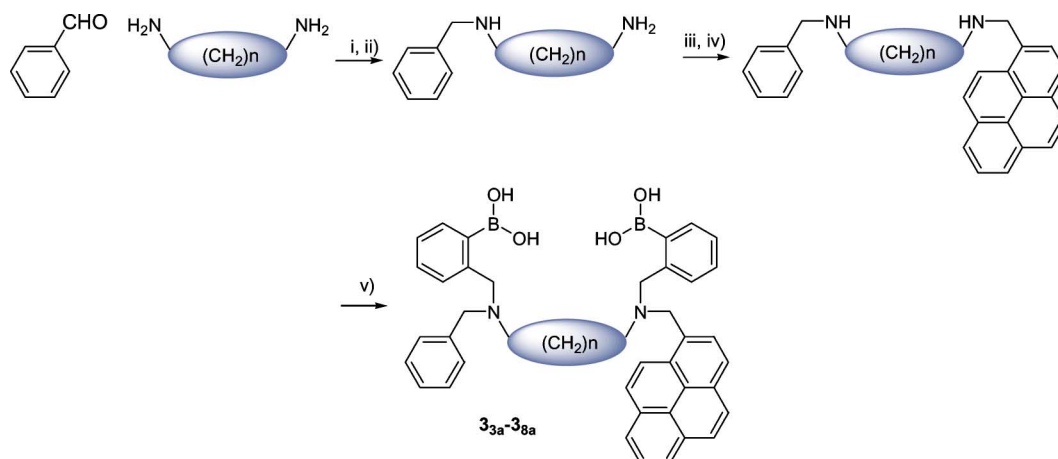


different core and fluorophore units, a modification that has resulted in systems where the selectivity and emission wavelength can be varied independently, a setup that had not been previously possible. This idea led us to adopt a modular approach when considering sensor design. Sensors were broken down into three subunits: receptor units, linker units and fluorophore units. The approach required the selection and synthesis of a set of molecular building blocks from which the fluorescent sensors could be easily constructed. The quick assembly of a diverse selection of fluorescent sensors required that the receptor and fluorophore units were linked to a core using the minimum number of synthetic linkage reactions. The use of common reactions meant that the synthetic routes towards new sensors would be convergent.

## LINKER DEPENDANCE

We first constructed the modular PET sensor **3<sub>6a</sub>** with two phenylboronic acid groups, because only through two point binding can saccharide selectivity be manipulated, a pyrene fluorophore and a hexamethylene linker. We began our investigations keeping the fluorophore constant (using pyrene throughout) and varied the linker from trimethylene (**3<sub>3a</sub>**) to octamethylene (**3<sub>8a</sub>**). This aim of this research was to elucidate the optimum linker length required for maximal D-glucose selectivity [38,39].

The synthesis of PET sensors **3<sub>3a</sub>-3<sub>8a</sub>** was achieved according to Scheme 1 from readily available starting materials. Monophenylboronic acid PET sensor **5<sub>a</sub>** was also prepared. To prepare monosubstituted alkyldiamines the reductive aminations were performed under high dilution conditions and with one equivalent of *p*-toluenesulphonic acid to every equivalent of alkyldiamine.



**Scheme 1.** Synthesis of PET sensors **3<sub>3a</sub>-3<sub>8a</sub>**. Reagents: i) *p*-Toluenesulphonic acid, THF/EtOH, ii) NaBH<sub>4</sub>, iii) 1-pyrenecarboxaldehyde, THF/MeOH, iv) NaBH<sub>4</sub>, v) 2-(2-bromobenzyl)-1,3,2-dioxaborinane, K<sub>2</sub>CO<sub>3</sub>, MeCN.

The fluorescence titrations of **3<sub>3a</sub>-3<sub>8a</sub>** and **5<sub>a</sub>** ( $1.0 \times 10^{-7}$  mol dm<sup>-3</sup>) with different saccharides were carried out in a pH 8.21 aqueous methanolic buffer solution [52.1 wt% methanol (KCl, 0.01000 mol dm<sup>-3</sup>; KH<sub>2</sub>PO<sub>4</sub>, 0.002752 mol dm<sup>-3</sup>; Na<sub>2</sub>HPO<sub>4</sub>, 0.002757 mol dm<sup>-3</sup>)] [40]. The fluorescence intensity of **3<sub>3a</sub>-3<sub>8a</sub>** and **5<sub>a</sub>** increased with increasing saccharide concentration. The observed stability constants (*K*) of PET sensors **3<sub>3a</sub>-3<sub>8a</sub>** and **5<sub>a</sub>** were calculated by fitting the emission intensity at 397 nm versus concentration and are given in Table I.

To help visualise the trends in the observed stability constants from Table I, the stability constants *K* of the diboronic acid sensors **3<sub>3a</sub>-3<sub>8a</sub>** are reported in Fig. 1 relative to the stability constants *K* of the equivalent monoboronic acid analogue **5<sub>a</sub>**. In most cases, the stability constants *K* with diboronic acid sensors **3<sub>3a</sub>-3<sub>8a</sub>** are higher than for the monoboronic acid sensor **5<sub>a</sub>**. Allosteric binding of the two boronic acid groups is clearly illustrated by the stabil-

ity constant differences between the mono- and diboronic acid compounds (sensors **5<sub>a</sub>** and **3<sub>3a</sub>-3<sub>8a</sub>** respectively).

In particular, it should be apparent from Fig. 1, that the stability constants *K* for diboronic acid sensors **3<sub>4a</sub>-3<sub>8a</sub>** with D-glucose and D-galactose are far greater than with the monoboronic acid sensor **5<sub>a</sub>**. Whereas the stability constant *K* of diboronic acid sensors **3<sub>4a</sub>-3<sub>8a</sub>** with D-fructose and D-mannose are, at most, twice as strong as with the monoboronic acid sensor **5<sub>a</sub>**. These results are not surprising since D-glucose and D-galactose will bind to diboronic acids readily at two sets of diols to form stable, cyclic 1:1 complexes. Conversely, each D-fructose and D-mannose molecule will only bind to diboronic acids through one diol to form 2:1 complexes. This 2:1 binding yields relative stability constants of ca. 2, as we are essentially witnessing the binding of a saccharide to a monoboronic acid twice, without the favourable increase in stability associated with cooperative binding.

**Table I.** The Quantum Yield  $q_{FM}$  for Molecular Sensors **3<sub>3a</sub>-3<sub>8a</sub>** and **5<sub>a</sub>** in the Absence of Saccharides and the Stability Constant *K* (Determination of Coefficient;  $r^2$ ) and Fluorescence Enhancement for the Monosaccharide Complexes of Molecular Sensors **3<sub>3a</sub>-3<sub>8a</sub>** and **5<sub>a</sub>**<sup>a</sup>

Sensor	$q_{FM}$	D-Glucose		D-Galactose		D-Fructose		D-Mannose	
		<i>K</i> (dm <sup>3</sup> mol <sup>-1</sup> )	Fluorescence enhancement	<i>K</i> (dm <sup>3</sup> mol <sup>-1</sup> )	Fluorescence enhancement	<i>K</i> (dm <sup>3</sup> mol <sup>-1</sup> )	Fluorescence enhancement	<i>K</i> (dm <sup>3</sup> mol <sup>-1</sup> )	Fluorescence enhancement
<b>3<sub>3a</sub></b>	0.16	103 ± 3 (1.00)	3.9	119 ± 5 (1.00)	3.5	95 ± 9 (0.99)	3.6	45 ± 4 (1.00)	2.7
<b>3<sub>4a</sub></b>	0.16	295 ± 11 (1.00)	3.3	222 ± 17 (1.00)	3.7	266 ± 28 (0.99)	4.2	39 ± 1 (1.00)	3.4
<b>3<sub>5a</sub></b>	0.20	333 ± 27 (1.00)	3.4	177 ± 15 (1.00)	3.0	433 ± 19 (1.00)	3.4	48 ± 2 (1.00)	3.0
<b>3<sub>6a</sub></b>	0.24	962 ± 70 (0.99)	2.8	657 ± 39 (1.00)	3.1	784 ± 44 (1.00)	3.2	74 ± 3 (1.00)	2.8
<b>3<sub>7a</sub></b>	0.16	336 ± 30 (0.98)	3.0	542 ± 41 (0.99)	2.9	722 ± 37 (1.00)	3.3	70 ± 5 (1.00)	2.7
<b>3<sub>8a</sub></b>	0.19	368 ± 21 (1.00)	2.3	562 ± 56 (0.99)	2.3	594 ± 56 (0.99)	2.3	82 ± 3 (1.00)	2.2
<b>5<sub>a</sub></b>	0.17	44 ± 3 (1.00)	4.5	51 ± 2 (1.00)	4.2	395 ± 11 (1.00)	3.6	36 ± 1 (1.00)	3.7

<sup>a</sup>The *K* values were analysed in Kaleida Graph using nonlinear (Levenberg-Marquardt algorithm) curve fitting. The errors reported are the standard errors obtained from the best fit.

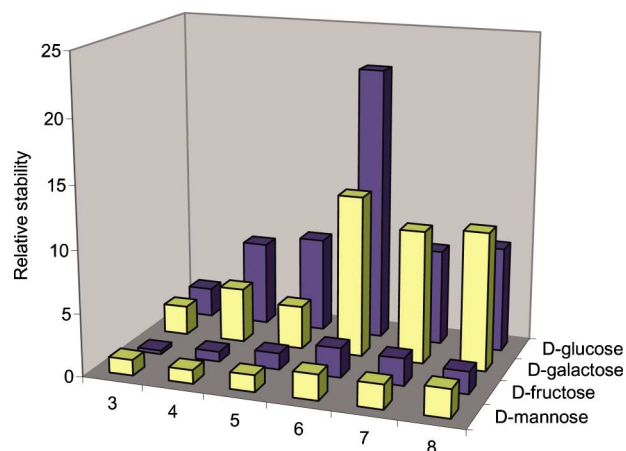


Fig. 1. Relative stability of 3<sub>3a</sub>-3<sub>8a</sub> compared to 5<sub>a</sub> with saccharides.

Sensor 3<sub>6a</sub> has the highest stability constant  $K$  with D-glucose amongst any of the sensors 5<sub>a</sub> and 3<sub>3a</sub>-3<sub>8a</sub>. This result ties in nicely with the results obtained with sensor 2, the nitrogens in sensor 2 are separated by six carbons while 3<sub>6a</sub> has a hexamethylene linker.

The stability constants  $K$  for the diboronic acid sensors 3<sub>7a</sub> and 3<sub>8a</sub> with D-galactose are larger than the stability constants  $K$  for the diboronic acid sensors 3<sub>7a</sub> and 3<sub>8a</sub> with D-glucose. The structures of D-glucose and D-galactose are shown in Fig. 2. The 1, 2- and 4, 6- diols of D-glucose point in the same direction (down), but in D-galactose the 1,2-diol is down and the 4,6-diol is up. The inter-diol distances of D-glucose are also shorter than those of D-galactose. Therefore, it is reasonable to predict that shorter linkers will favour D-glucose and longer linkers will favour D-galactose binding. This is the observed trend as shown in Fig. 1.<sup>3</sup> Sensors 3<sub>3a</sub>-3<sub>6a</sub>, all show higher relative affinity for D-glucose. Whilst sensors 3<sub>7a</sub> and 3<sub>8a</sub> display higher relative affinity for D-galactose. What is also evident from Fig. 1 is that a hexamethylene linker (3<sub>6a</sub>) provides optimum spacing for maximal D-glucose selectivity within our systems.

## LINKER DEPENDENCE AND DISACCHARIDES

When compared to monosaccharide receptors only a small number of synthetic receptors for disaccharides [44–47] and oligosaccharides [10, 48–55] currently exist.

<sup>3</sup> It should be noted that ascertaining the exact structures of boronic acid-saccharide complexes is non-trivial. In indicating the hydroxy groups at the 1,2 and 4,6 positions of D-glucose and D-galactose as suitable binding sites for diboronic acids we are contemplating a model considered valid only as an initial complex of the  $\alpha$ -D-pyranose form of the saccharide under non-aqueous conditions. For further information on this point, we would direct the reader to the binding studies carried out by Norrild and Eggert [14, 41–43].

One reason is the problem associated with positioning the two binding sites to create a selective receptor for these larger and more flexible saccharides.

Following our investigation into the effect of linker length on monosaccharides, we decided to probe the effect of the linker length on selected disaccharides [56].

The fluorescence titrations of 3<sub>3a</sub>-3<sub>8a</sub> and 5<sub>a</sub> ( $1.0 \times 10^{-7}$  mol dm<sup>-3</sup>,  $\lambda_{\text{ex}} = 342$  nm) with different saccharides, were carried out in a pH 8.21 aqueous methanolic buffer solution, as described above. The fluorescence intensity of 3<sub>3a</sub>-3<sub>8a</sub> and 5<sub>a</sub> increased with increasing saccharide concentration. The stability constants  $K$  of PET sensors 3<sub>3a</sub>-3<sub>8a</sub> and 5<sub>a</sub> were calculated by fitting the emission intensity at 397 nm versus concentration of saccharide curves. Fluorescence enhancements were calculated by the same method. Where the emission intensity at 397 nm versus concentration of saccharide curves failed to describe a distinct plateau the maximum observed fluorescence enhancements were reported. Stability constants  $K$  and fluorescence enhancements are given in Table II. The stability constants  $K$  of the diboronic acid sensors 3<sub>3a</sub>-3<sub>8a</sub> and 5<sub>a</sub> with saccharides are displayed in Fig. 4 and Fig. 5.

It has been previously shown from NMR and fluorescence studies that phenylboronic acids have a strong preference to bind with the hydroxyls of saccharides in their furanose forms [14, 41–43, 57]. Monosaccharides and many disaccharides can isomerise between their pyranose and furanose forms in aqueous solvents. The aqueous methanolic buffer used for the fluorescence runs allows for this isomerisation. As shown in Fig. 4 and Fig. 6, D-melibiose ( $\alpha$ -D-Galp-(1→6)-D-Glc) and D-lactulose ( $\beta$ -D-Galp-(1→4)-D-Fru) can interconvert between their pyranose and furanose forms. By comparison D-maltose ( $\alpha$ -D-Glcp-(1→4)-D-Glc) and D-leucrose ( $\alpha$ -D-Glcp-(1→5)-D-Fru) are disaccharides linked to the 4th carbon (as numbered from the anomeric centre) and as such they are conformationally fixed as pyranosides [58].

The increase in stability constant  $K$  for 3<sub>3a</sub>-3<sub>8a</sub> on binding to D-melibiose is significantly larger than the stability constant  $K$  observed for the reference compound 5<sub>a</sub>. The increase indicates that D-melibiose binds in a 1:1 ratio, like D-glucose, with the formation of a stable, cyclic structure. The stability constants  $K$  for 3<sub>3a</sub>-3<sub>8a</sub> with D-lactulose are at most double that of the reference compound 5<sub>a</sub>, indicating that D-lactulose, like D-fructose, binds to 3<sub>3a</sub>-3<sub>8a</sub> in a 2:1 ratio, forming an acyclic structure.

The selectivity trend displayed by 3<sub>3a</sub>-3<sub>8a</sub> towards D-melibiose mirrors that of D-glucose, which implies that 3<sub>3a</sub>-3<sub>8a</sub> is forming stable cyclic structures with the furanose ring segment of these saccharides.

The results indicated that binding with diboronic acid receptors occurs preferentially with disaccharides,

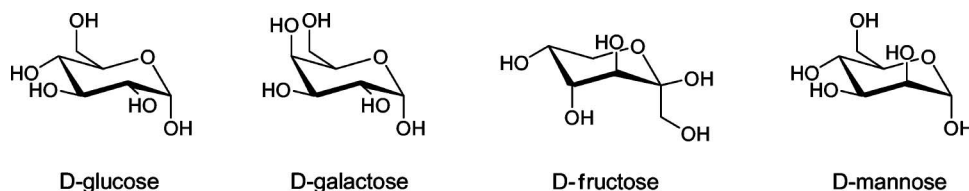


Fig. 2. Saccharide structures.

which can isomerise between their pyranose and furanose conformations. D-Melibiose, for instance, can isomerise into a glucofuranose form and displays enhanced binding with the D-glucose selective sensor **3**<sub>6a</sub>.

This gives us the ability not only to tune for specific terminal mono-saccharides appended to larger carbohydrates but also to distinguish between them by their linker position, a facet that could prove immensely useful in the field of glycobiology [1].

## FLUOROPHORE DEPENDENCE

Having determined the effect of the linker length on saccharide selectivity, we set out to probe the next variable component, the fluorophore. Although not directly involved in saccharide binding, the nature of the fluorophore directly influences both the solvation and steric crowding of the binding site.

Diboronic acid PET sensors **3**<sub>6a</sub>-**3**<sub>6e</sub> and monoboronic acid PET sensors **5**<sub>a</sub>-**5**<sub>e</sub> were synthesised according to Scheme 2 from readily available starting materials. The synthesis allows for the facile preparation of diboronic acid PET sensors appended with a range of different fluorophores [59].

The fluorescence titrations of **3**<sub>6a</sub>-**3**<sub>6e</sub> and **5**<sub>a</sub>-**5**<sub>e</sub> with different saccharides were carried out in a pH 8.21 aqueous methanolic buffer solution, as described above. The fluorescence intensity of **3**<sub>6a</sub>-**3**<sub>6e</sub> increased with increasing

saccharide concentration. The observed stability constants *K* of PET sensors **3**<sub>6a</sub>-**3**<sub>6e</sub> and **5**<sub>a</sub>-**5**<sub>e</sub> were calculated by the fitting of emission intensity versus saccharide concentration curves and are reported in Table III.

To help visualise the trends in the observed stability constants *K* in Table III the stability constants *K* of the diboronic acid sensors **3**<sub>6a</sub>-**3**<sub>6e</sub> are reported in Fig. 7 relative to the stability constants *K* of the equivalent monoboronic acid analogues **5**<sub>a</sub>-**5**<sub>e</sub>. Once again the relative stabilities clearly illustrate that an increase in selectivity is obtained by cooperative binding through the formation of 1:1 cyclic systems. The large enhancement of the relative stability observed for the 1:1 cyclic systems (D-glucose and D-galactose) are clearly contrasted with the small two fold enhancement observed for the 2:1 acyclic systems (D-fructose and D-mannose).

The largest enhancements in stability are by **3**<sub>6a</sub> and **3**<sub>6e</sub> the pyrene and 2-naphthalene appended sensors, with **3**<sub>a</sub> exhibiting enhanced D-glucose selectivity and **3**<sub>6e</sub> exhibiting enhanced D-galactose selectivity.

Sensor **3**<sub>a</sub> contains a pyrene moiety, which is the largest  $\pi$ -surface in this series. Sensor **3**<sub>6a</sub> displays the greatest enhancement in selectivity for D-glucose over D-galactose. By reducing the size of the hydrophobic  $\pi$ -surface, as with **3**<sub>6d</sub> and **3**<sub>6e</sub>, (appended with 1- and 2-naphthalene), the selectivity for the monosaccharides switches from D-glucose to D-galactose. Since, the size of the  $\pi$ -surface affects the solvation of the receptor, the

**Table II.** Stability Constant *K* (Determination of Coefficient,  $r^2$ ) and Fluorescence Enhancement for the Disaccharide Complexes of Molecular Sensors **3**<sub>3a</sub>-**3**<sub>8a</sub> and **5**<sub>a</sub><sup>a</sup>

Sensor	D-Melibiose		D-Maltose		D-Lactulose		D-Leucrose	
	<i>K</i> (dm <sup>3</sup> mol <sup>-1</sup> )	Fluorescence enhancement	<i>K</i> (dm <sup>3</sup> mol <sup>-1</sup> )	Fluorescence enhancement	<i>K</i> (dm <sup>3</sup> mol <sup>-1</sup> )	Fluorescence enhancement	<i>K</i> (dm <sup>3</sup> mol <sup>-1</sup> )	Fluorescence enhancement
<b>3</b> <sub>3a</sub>	33 ± 7 (0.98)	2.4	0 ± 2 (0.96)	1.5 <sup>b</sup>	126 ± 14 (0.99)	3.5	29 ± 3 (0.99)	2.5 <sup>b</sup>
<b>3</b> <sub>4a</sub>	77 ± 9 (0.99)	4.9 <sup>b</sup>	31 ± 7 (0.98)	3.5 <sup>b</sup>	477 ± 92 (0.95)	4.5	35 ± 2 (1.00)	3.4 <sup>b</sup>
<b>3</b> <sub>5a</sub>	184 ± 11 (1.00)	3.8	2 ± 1 (0.99)	2.1 <sup>b</sup>	616 ± 114 (0.97)	5.0	41 ± 2 (1.00)	3.5 <sup>b</sup>
<b>3</b> <sub>6a</sub>	339 ± 17 (1.00)	2.9	52 ± 14 (0.98)	2.3	595 ± 30 (1.00)	3.2	69 ± 2 (1.00)	2.9 <sup>b</sup>
<b>3</b> <sub>7a</sub>	153 ± 4 (1.00)	3.3	5 ± 1 (1.00)	2.0 <sup>b</sup>	493 ± 28 (1.00)	3.3	21 ± 5 (0.97)	3.9 <sup>b</sup>
<b>3</b> <sub>8a</sub>	192 ± 30 (0.98)	2.9	22 ± 4 (0.98)	2.4 <sup>b</sup>	528 ± 29 (1.00)	2.6	72 ± 5 (1.00)	2.7 <sup>b</sup>
<b>5</b> <sub>a</sub>	96 ± 5 (1.00)	3.9	5 ± 1 (0.99)	2.1 <sup>b</sup>	473 ± 10 (1.00)	3.7	58 ± 3 (1.00)	3.7

<sup>a</sup>The *K* values were analysed in Kaleida Graph using nonlinear (Levenberg-Marquardt algorithm) curve fitting. The errors reported are the standard errors obtained from the best fit.

<sup>b</sup>Maximum observed fluorescence enhancement.

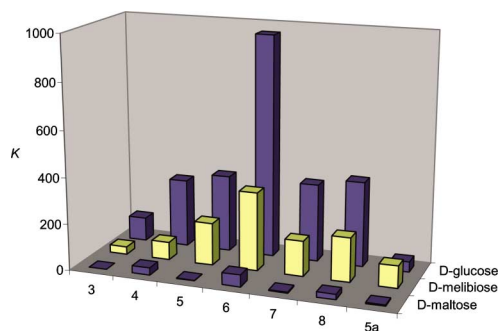


Fig. 3. Stability constants  $K$  of  $3_{3a}$ - $3_{8a}$  and  $5a$  with D-glucose and its derivatives.

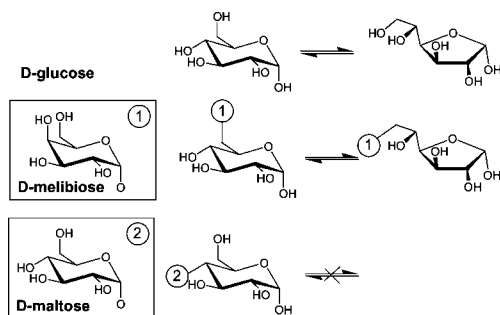


Fig. 4. Structure of D-glucose and its derivatives.

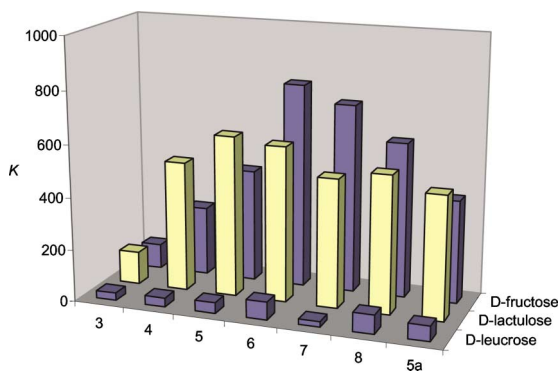


Fig. 5. Stability constants  $K$  of  $3_{3a}$ - $3_{8a}$  and  $5a$  with D-fructose and its derivatives.

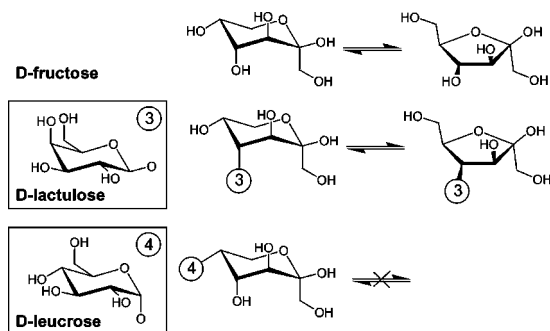


Fig. 6. Structure of D-fructose and its derivatives.

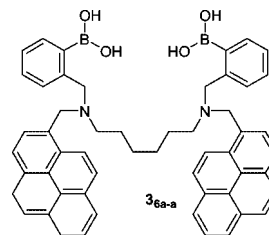
larger the  $\pi$ -surface the more hydrophobic the receptor. These results indicate that the best match between receptor and guest is for  $3_{6a}$ - $3_{6c}$  with D-glucose and  $3_{6d}$  and  $3_{6e}$  with D-galactose.

In interpreting these values however, the size of the fluorophore's  $\pi$ -surface must be considered in conjunction with the number of *peri*-hydrogens each fluorophore contains. Thus coupling the effects of solvation with the steric crowding induced at the binding site by the fluorophore. There is little difference between the size of 1-naphthalene's  $\pi$ -surface and that of 2-naphthalene. The same is true for phenanthrene and anthracene. In these cases, the observed trends are probably due to increased steric crowding at the binding site. In both cases, a decrease in the relative stability is coupled to an increase in the number of *peri*-hydrogens. Anthracene has 2 *peri*-hydrogens, more than any other fluorophore in the series and clearly displays the lowest relative stability. It is not surprising that increasing the steric crowding of the receptor site reduces binding efficiency.

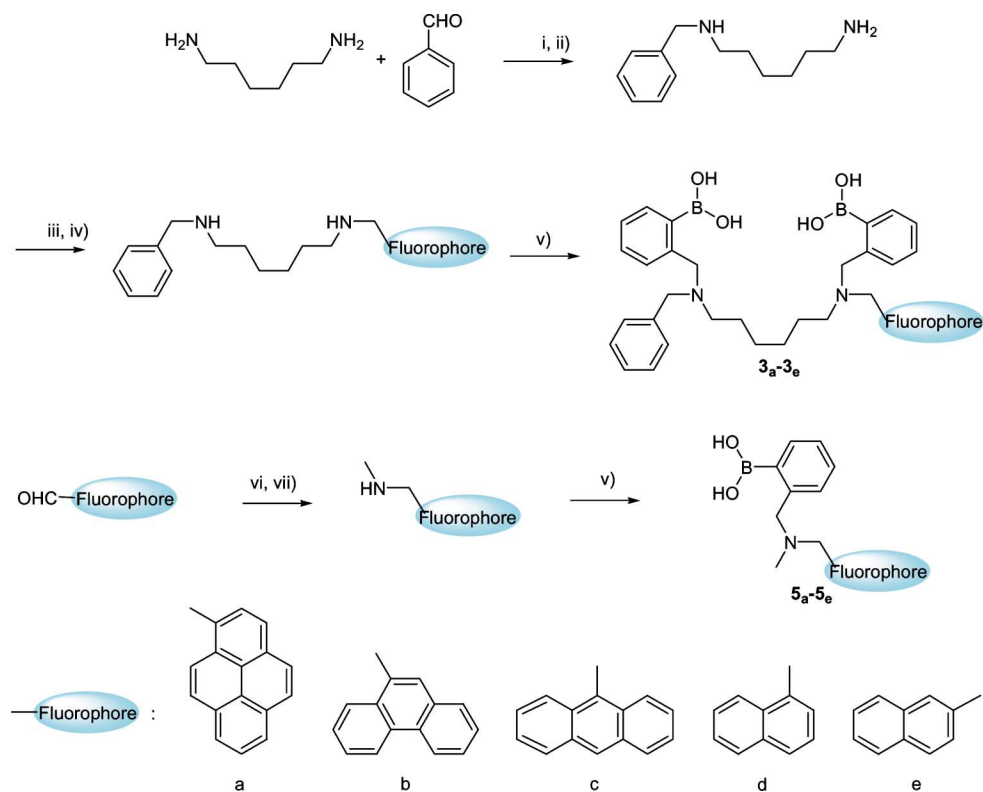
These results demonstrate that in a PET saccharide sensor with two phenylboronic acid groups, a hexamethylene linker and a fluorophore, the choice of the fluorophore is crucial. Selectivity is fluorophore dependent and careful choice of the fluorophore, such that it complements the polarity of the chosen guest species, is imperative. As well as considering solubility, minimizing the steric repulsions from *peri*-hydrogens not only increases the relative stability but can also be used to fine tune sensitivity toward specific saccharides.

## MULTIPLE FLUOROPHORES AND EXCIMER EMISSION

Consideration of the boronic acid receptor's separation, as well as the solvation and steric crowding at the binding site, establishes that a hexamethylene linker and a pyrene fluorophore provide the best D-glucose selectivity from the combination of components tried. With this in mind we examined the effects of adding multiple fluorophores to the system.



Sensor  $3_{6a-a}$  has been previously reported [60]. The molecule was re-synthesised but the fluorescence titrations



**Scheme 2.** i) Benzaldehyde, *p*-toluenesulfonic acid, THF/EtOH, ii) NaBH<sub>4</sub>, iii) fluorophore-aldehyde, THF/MeOH, iv) NaBH<sub>4</sub> v) 2-(2-bromobenzyl)-1,3,2-dioxaborinane, K<sub>2</sub>CO<sub>3</sub>, MeCN, vi) methylamine, THF/MeOH, vii) NaBH<sub>4</sub>.

of **3<sub>6a-a</sub>** ( $7.5 \times 10^{-7}$  mol dm<sup>-3</sup>,  $\lambda_{\text{ex}} = 342$  nm) with different saccharides, were carried out in a pH 8.21 aqueous methanolic buffer solution, as described above. The synthetic procedure will be published elsewhere. The fluorescence intensity of **3<sub>6a-a</sub>** increased with increasing saccharide concentration. The observed stability constants *K* of PET sensor **3<sub>6a-a</sub>** were calculated by the fitting of

emission intensity versus saccharide concentration curves and are reported in Table IV. The stability constants *K* show that while the selectivity order remains unchanged, the binding is reduced across the board 3–4 fold by the introduction of a second pyrene moiety. Given the increase in steric crowding at the binding site and the particularly hydrophobic nature of this compound due to its two large

**Table III.** Stability Constant *K* (Determination of Coefficient,  $r^2$ ) and Fluorescence Enhancement for the Saccharide Complexes of Molecular Sensors **3<sub>6a-3<sub>6e</sub></sub>** and **5<sub>a-5<sub>e</sub></sub>**<sup>a</sup>

Sensor	D-Glucose		D-Galactose		D-Fructose		D-Mannose	
	<i>K</i> (dm <sup>3</sup> mol <sup>-1</sup> )	Fluorescence enhancement	<i>K</i> (dm <sup>3</sup> mol <sup>-1</sup> )	Fluorescence enhancement	<i>K</i> (dm <sup>3</sup> mol <sup>-1</sup> )	Fluorescence enhancement	<i>K</i> (dm <sup>3</sup> mol <sup>-1</sup> )	Fluorescence enhancement
<b>3<sub>6a</sub></b>	962 ± 70 (0.99)	2.8	657 ± 39 (1.00)	3.1	784 ± 44 (1.00)	3.2	74 ± 3 (1.00)	2.8
<b>5<sub>a</sub></b>	44 ± 3 (1.00)	4.5	51 ± 2 (1.00)	4.2	395 ± 11 (1.00)	3.6	36 ± 1 (1.00)	3.7
<b>3<sub>6b</sub></b>	325 ± 58 (0.97)	1.5	611 ± 101 (0.97)	1.4	1013 ± 126 (0.98)	1.4	134 ± 18 (0.98)	1.4
<b>5<sub>b</sub></b>	30 ± 7 (0.98)	1.5	77 ± 12 (0.98)	1.4	548 ± 55 (0.99)	1.4	58 ± 8 (0.98)	1.4
<b>3<sub>6c</sub></b>	441 ± 76 (0.98)	3.2	536 ± 31 (1.00)	3.1	1000 ± 69 (0.99)	3.0	111 ± 6 (1.00)	2.8
<b>5<sub>c</sub></b>	61 ± 3 (1.00)	3.4	93 ± 6 (1.00)	3.0	713 ± 35 (1.00)	3.0	61 ± 3 (1.00)	3.0
<b>3<sub>6d</sub></b>	417 ± 60 (0.98)	6.1	1072 ± 68 (0.99)	5.4	964 ± 41 (1.00)	5.5	101 ± 3 (1.00)	5.0
<b>5<sub>d</sub></b>	52 ± 1 (1.00)	5.7	78 ± 5 (1.00)	5.0	529 ± 45 (0.99)	5.4	46 ± 1 (1.00)	5.2
<b>3<sub>6e</sub></b>	532 ± 57 (0.99)	4.2	894 ± 66 (0.99)	4.1	1068 ± 63 (1.00)	3.8	98 ± 4 (1.00)	3.5
<b>5<sub>e</sub></b>	35 ± 2 (1.00)	4.5	49 ± 4 (1.00)	4.3	399 ± 34 (0.99)	4.6	40 ± 2 (1.00)	3.8

<sup>a</sup>The *K* values were analysed in Kaleida Graph using nonlinear (Levenberg-Marquardt algorithm) curve fitting. The errors reported are the standard errors obtained from the best fit.

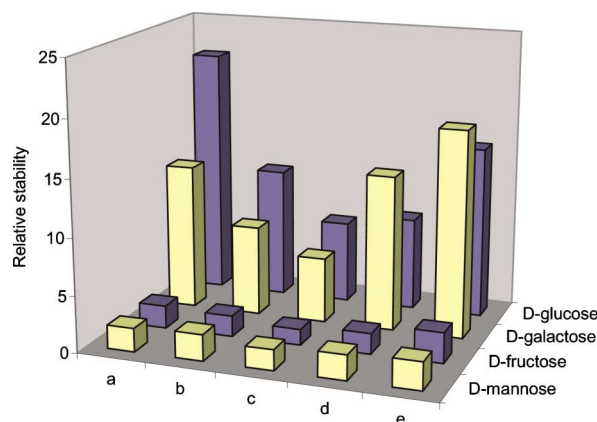


Fig. 7. Relative stability of  $3_{6a}$ - $3_{6e}$  compared to  $5_a$ - $5_e$  with saccharides.

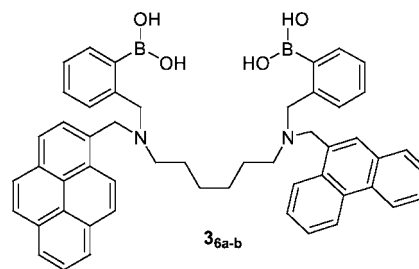
fluorophore moieties, this is consistent with our previous results.

In addition, it was also possible to observe the long wavelength excimer emission due to  $\pi$ - $\pi$  stacking of the pyrene fluorophores around 470 nm. This fluorescence emission has somewhat more modest intensity than the main emission observed at 397 nm. Nevertheless, as D-glucose binds to the receptor it forms a rigid 1:1 cyclic structure and in so doing increases the proximity of the boronic acids. This interaction forces the separation between the two pyrene fluorophores to increase, leading to reduced  $\pi$ - $\pi$  interactions between them. This change in orientation of the system's components manifests itself in the fluorescence emission spectrum as a clear decrease in excimer emission intensity with added saccharide.

## MULTIPLE FLUOROPHORES, EXCIMER EMISSION AND ENERGY TRANSFER

Whilst systems appended with multiple fluorophores suffer from reduced binding constants, there are some

advantages that can be obtained from using multiple fluorophores, namely the process of energy transfer.



Fluorescence energy transfer is the transfer of excited-state energy from a donor to an acceptor. The transfer occurs as a result of transition dipole-dipole interactions between the donor-acceptor pair [61]. We reported the fluorescent sensor  $3_{6a-b}$  that had two phenylboronic acid groups a hexamethylene linker and two different fluorophore groups (phenanthrene and pyrene) [62]. Our idea with the system was to investigate the efficiency of energy transfer (ET) from phenanthrene to pyrene as a function of saccharide binding. A similar concept had previously been employed in the construction of a fluorescent calix[4]arene sodium sensor [63]. The excitation and emission wavelengths of the phenanthrene (donor) are 299 and 369 nm, respectively, while the excitation and emission wavelengths of the pyrene (acceptor) are 342 and 397/417 nm, respectively. The emission wavelength of phenanthrene (369 nm) and excitation wavelength of pyrene (342 nm) overlap. These observations led us to postulate that intramolecular energy transfer from phenanthrene to pyrene could take place in  $3_{6a-b}$ . As in the pyrene-pyrene appended system  $3_{6a-a}$  it was possible to observe the long wavelength excimer emission, this time due to  $\pi$ - $\pi$  stacking of phenanthrene and pyrene in  $3_{6a-b}$ .

Table IV. Stability Constant  $K$  (Coefficient of Determination;  $r^2$ ) and Fluorescence Enhancement for the Saccharide Complexes of Molecular Sensors  $3_{6a-a}$  and  $3_{6a-b}$ <sup>a</sup>

Sensor	D-Glucose		D-Galactose		D-Fructose		D-Mannose	
	$K$ (dm <sup>3</sup> mol <sup>-1</sup> )	Fluorescence enhancement	$K$ (dm <sup>3</sup> mol <sup>-1</sup> )	Fluorescence enhancement	$K$ (dm <sup>3</sup> mol <sup>-1</sup> )	Fluorescence enhancement	$K$ (dm <sup>3</sup> mol <sup>-1</sup> )	Fluorescence enhancement
$3_{6a-a}$	260 ± 15 (1.00)	4.9	237 ± 6 (1.00)	4.2	244 ± 26 (0.99)	3.4	32 ± 3 (0.99)	3.2
$3_{6a-b}^b$	142 ± 12 (0.99)	3.9	74 ± 7 (0.99)	2.2	76 ± 10 (0.98)	1.7	<sup>c</sup>	<sup>c</sup>
$3_{6a-b}^d$	108 ± 10 (0.99)	2.4	81 ± 8 (0.99)	2.6	125 ± 11 (0.99)	3.5	8 ± 1 (1.00)	3.5

<sup>a</sup>The  $K$  values were analysed in KaleidaGraph using nonlinear (Levenberg-Marquardt algorithm) curve fitting. The errors reported are the standard errors obtained from the best fit.

<sup>b</sup> $\lambda_{ex}$  = 299 nm,  $\lambda_{em}$  = 417 nm.

<sup>c</sup>The  $K$  and fluorescence enhancement could not be determined because of the small changes in fluorescence.

<sup>d</sup> $\lambda_{ex}$  = 342 nm,  $\lambda_{em}$  = 417 nm.

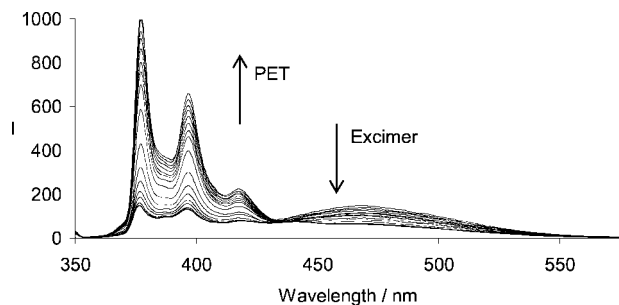


**Fig. 8.** Fluorescence emission spectrum of  $3_{6a-a}$  ( $7.5 \times 10^{-6}$  mol dm $^{-3}$ ) with increasing amounts of D-glucose (from 0 to  $1.0 \times 10^{-1}$  mol dm $^{-3}$ ) in 52.1 wt% MeOH pH 8.21 phosphate buffer.  $\lambda_{ex} = 342$  nm.

To confirm that the  $\pi$ - $\pi$  stacking of sensor  $3_{6a-b}$  was only intramolecular and not intermolecular we plotted the absorption versus concentration of both  $3_{6a-b}$  and  $5_a + 5_b$  in pH 8.21 aqueous methanolic buffer solutions, as described above for the fluorescence titrations. The plots for sensor  $3_{a-b}$  and the mixture of sensors  $5_a + 5_b$  were linear until  $2.0 \times 10^{-5}$  mol dm $^{-3}$  [ $\epsilon = 2.12 \times 10^4$  dm $^3$  mol $^{-1}$  ( $\lambda_{max} = 342$  nm) for sensor  $3_{6a-b}$  and  $\epsilon = 4.59 \times 10^4$  dm $^3$  mol $^{-1}$  ( $\lambda_{max} = 342$  nm) for sensors  $5_a + 5_b$ ], clearly demonstrating that the  $\pi$ - $\pi$  stacking of sensor  $3_{a-b}$  is only intramolecular.

The fluorescence titrations of  $3_{6a-b}$  ( $2.5 \times 10^{-6}$  mol dm $^{-3}$ ,  $\lambda_{ex} = 299$  nm for phenanthrene and  $\lambda_{ex} = 342$  nm for pyrene) with different saccharides were carried out in a pH 8.21 aqueous methanolic buffer, as described above. The fluorescence intensity of sensor  $3_{6a-b}$  at 417 nm increased with added saccharide when excited at both 299 and 342 nm, while the excimer emission at 460 nm decreased with added saccharide. The excimer emission change indicates that the fluorophore stacking of phenanthrene and pyrene is broken on saccharide binding.

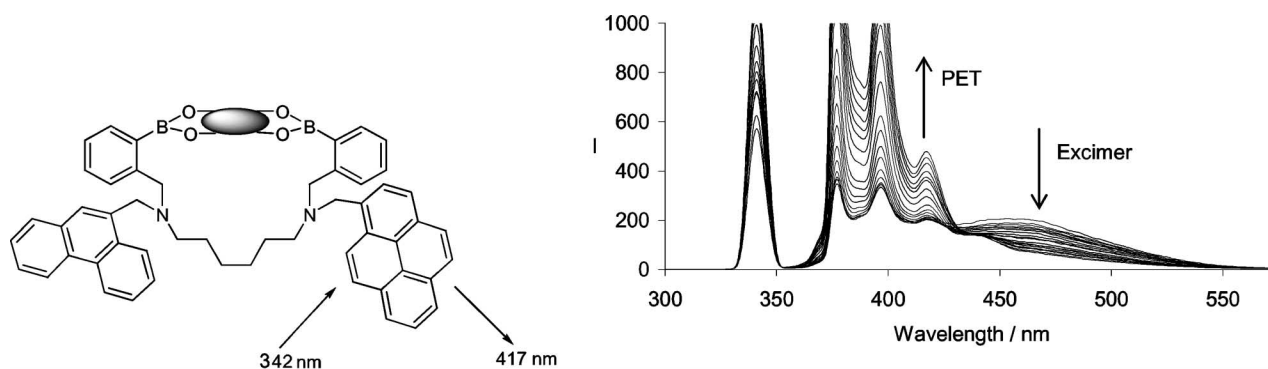


**Fig. 9.** D-Glucose binding to  $3_{6a-b}$  inhibits PET, restoring fluorescence. The increased separation of the fluorophores prevents  $\pi$ - $\pi$  stacking, diminishing excimer emission. *Left.* Schematic representation. *Right.* Fluorescence intensity versus wavelength for  $3_{6a-b}$  ( $2.5 \times 10^{-6}$  mol dm $^{-3}$ ) displaying photoinduced electron transfer and excimer emission with increasing concentrations of D-glucose (from 0 to  $1.0 \times 10^{-1}$  mol dm $^{-3}$ ) in 52.1 wt% MeOH pH 8.21 phosphate buffer.  $\lambda_{ex} = 342$  nm.

When phenanthrene was excited at 299 nm the fluorescence emission spectrum did not display emission at 369 nm (as would be expected for phenanthrene) but rather displayed an emission spectrum characteristic of pyrene with an emission maximum at 417 nm. The result demonstrating that energy transfer from phenanthrene to pyrene had indeed occurred.

The stability constants  $K$  of sensors  $3_{6a-b}$  with ( $\lambda_{ex} = 299$  nm), and  $3_{6a-b}$  ( $\lambda_{ex} = 342$  nm) were calculated by fitting the emission and intensity at 417 nm versus concentration of saccharide curves and are given in Table IV. The stability constants  $K$  for diboronic acid sensor  $3_{6a-b}$  ( $\lambda_{ex} = 299$  and 342 nm) with D-glucose were enhanced relative to those of monoboronic acid sensors  $5_a$  and  $5_b$ , while the stability constants  $K$  for diboronic acid sensor  $3_{6a-b}$  ( $\lambda_{ex} = 299$  and 342 nm) with D-fructose were reduced relative to those for monoboronic acid sensors  $5_a$  and  $5_b$ .

Sensor  $3_{6a-b}$  was particularly noteworthy in that the difference between the observed fluorescence enhancements obtained when excited at phenanthrene ( $\lambda_{ex} = 299$  nm) and pyrene ( $\lambda_{ex} = 342$  nm) can be correlated with the molecular structure of the saccharide-sensor complex, see Table IV. The fluorescence enhancement of sensor  $3_{6a-b}$  with D-glucose was 3.9 times greater when excited at 299 nm and 2.4 times greater when excited at 342 nm. Whereas, with D-fructose the enhancement was 1.9 times greater when excited at 299 nm and 3.2 times greater when excited at 342 nm. This is to say that the selectivity between D-fructose and D-glucose within the same complex is in fact inverted dependant on the excitation wavelength used, this is clearly displayed in Fig. 11 and Fig. 12. The results derive from the fact that energy transfer from phenanthrene to pyrene in the 1:1 cyclic diboronic acid-saccharide complex is far more

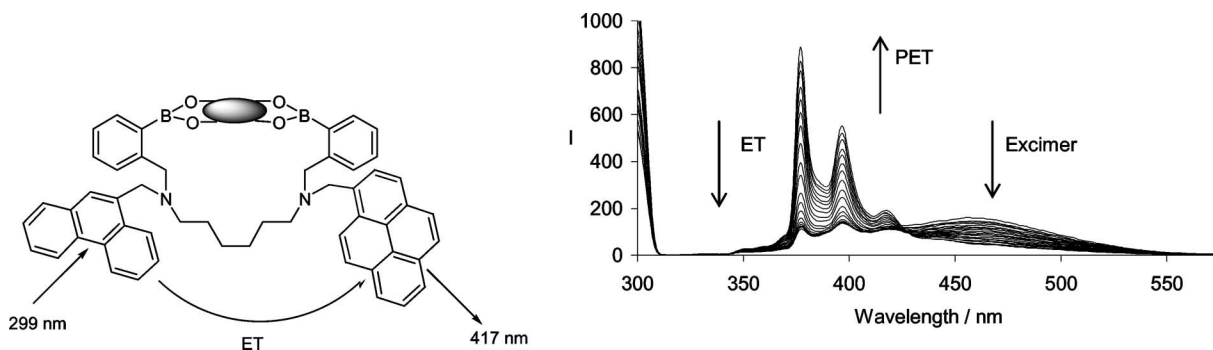


**Fig. 10.** D-Glucose binding to  $3_{6a-b}$  inhibits PET, restoring fluorescence. The compound's conformation allows ET to operate and the increased separation of the fluorophores prevents  $\pi$ - $\pi$  stacking, diminishing excimer emission. *Left.* Schematic representation. *Right.* Fluorescence intensity versus wavelength for  $3_{6a-b}$  ( $2.5 \times 10^{-6} \text{ mol dm}^{-3}$ ) displaying energy transfer, photoinduced electron transfer and excimer emission with increasing concentrations of D-glucose (from 0 to  $1.0 \times 10^{-1} \text{ mol dm}^{-3}$ ) in 52.1 wt% MeOH pH 8.21 phosphate buffer.  $\lambda_{\text{ex}} = 299 \text{ nm}$ .

efficient than the alternative 2:1 acyclic complex. This approach allows for pertinent discrimination between saccharides based on their binding motif (*i.e.* the formation of a 1:1 or a 2:1 complex) with diboronic acid receptors.

## CONCLUSION

Using simple building blocks we have synthesised a string of molecular sensors. Rational alterations of the sensor's constituent parts have afforded information on the effects of receptor spacing, of solvation and steric crowding, and of how to utilise the different binding motifs to identify them. In the case of monosaccharides both the observed stability constants and the fluorescence enhancements displayed by the sensors, have demonstrated that

the use of a hexamethylene linker and a single pyrene fluorophore achieve good D-glucose selectivity. In the case of disaccharides the capacity exists to tune for specific terminal monosaccharides appended to larger carbohydrates, as well as distinguishing between them by their linker positions.

Though the binding constants  $K$  are reduced, appending multiple fluorophores to modular systems offers the distinct advantage of allowing energy transfer mechanisms to operate. This significantly enhances the selectivity for complexes formed in a 1:1 cyclic manner. Future research will study the effects of energy transfer systems in which the fluorophores have been removed from the proximity of the binding pocket, thus circumventing the issue of unfavourable steric crowding and hydrophobic effects at the binding pocket, whilst retaining enhanced saccharide selectivity.

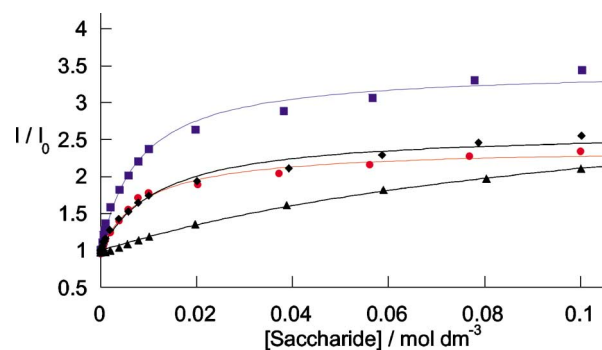


**Fig. 11.** Relative fluorescence intensity versus saccharide concentration profile of  $3_{6a-b}$  ( $2.5 \times 10^{-6} \text{ mol dm}^{-3}$ ) displaying PET at the pyrene fluorophore with (●) D-glucose, (■) D-fructose, (◆) D-galactose, (▲) D-mannose, in 52.1 wt% MeOH pH 8.21 phosphate buffer.  $\lambda_{\text{ex}} = 342 \text{ nm}$ ,  $\lambda_{\text{em}} = 417 \text{ nm}$ .

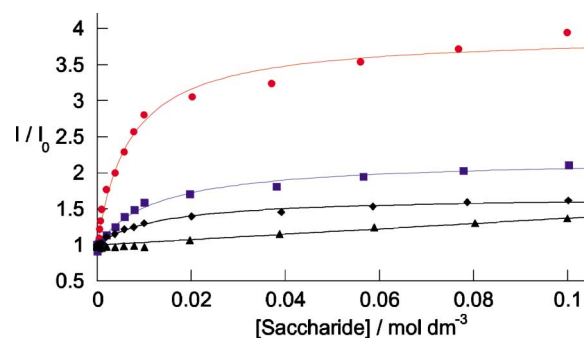


**Fig. 12.** Relative fluorescence intensity versus saccharide concentration profile of  $3_{6a-b}$  ( $2.5 \times 10^{-6} \text{ mol dm}^{-3}$ ) displaying ET between the phenanthrene and pyrene fluorophores with (●) D-glucose, (■) D-fructose, (◆) D-galactose, (▲) D-mannose, in 52.1 wt% MeOH pH 8.21 phosphate buffer.  $\lambda_{\text{ex}} = 299 \text{ nm}$ ,  $\lambda_{\text{em}} = 417 \text{ nm}$ .

## REFERENCES

1. S. Hurlley, R. Service, and P. Szuromi (2001). *Science* **291**, 2337.
2. T. D. James and S. Shinkai (2002). *Top. Curr. Chem.* **218**, 159–200.
3. J. H. Hartley, T. D. James, and C. J. Ward (2000). *J. Chem. Soc. Perkin Trans. 1* 3155–3184.
4. A. P. de Silva, H. Q. N. Gunaratne, T. Gunnlaugsson, A. J. M. Huxley, C. P. McCoy, J. T. Rademacher, and T. E. Rice (1997). *Chem. Rev.* **97**, 1515–1566.
5. A. P. Davis and R. S. Wareham (1999). *Angew. Chem. Int. Ed. Engl.* **38**, 2978–2996.
6. M. Granda-Valdes, R. Badia, G. Pina-Luis, and M. E. Diaz-Garcia (2000). *Quim. Anal.* **19**, 38–53.
7. A. W. Czarnik (1993). *Fluorescent Chemosensor for Ion and Molecular Recognition*, American Chemical Society Books, Washington.
8. W. Wang, X. Gao, and B. Wang (2002). *Curr. Org. Chem.* **6**, 1285–1317.
9. W. Yang, H. He, and D. G. Drucehammer (2001). *Angew. Chem. Int. Ed. Engl.* **40**, 1714–1718.
10. Z. Zhong and E. V. Anslyn (2002). *J. Am. Chem. Soc.* **124**, 9014–9015.
11. A. J. Tong, A. Yamauchi, T. Hayashita, Z. Y. Zhang, B. D. Smith, and N. Teramae (2001). *Anal. Chem.* **73**, 1530–1536.
12. N. DiCesare and J. R. Lakowicz (2001). *Chem. Commun.* 2022–2023.
13. H. Cao, D. I. Diaz, N. DiCesare, J. R. Lakowicz, and M. D. Heagy (2002). *Org. Lett.* **4**, 1503–1505.
14. H. Eggert, J. Frederiksen, C. Morin, and J. C. Norrild (1999). *J. Org. Chem.* **64**, 3846–3852.
15. T. D. James, K. R. A. S. Sandanayake, and S. Shinkai (1996). *Angew. Chem. Int. Ed. Engl.* **35**, 1911–1922.
16. T. D. James, K. R. A. S. Sandanayake, and S. Shinkai (1995). *Nature* **374**, 345–347.
17. S. Striegler (2003). *Curr. Org. Chem.* **7**, 81–102.
18. J. T. Suri, D. B. Cordes, F. E. Cappuccio, R. A. Wessling, and B. Singaram (2003). *Langmuir* **19**, 5145–5152.
19. S. De Marchi, E. Cecchin, A. Basil, G. Proto, W. Donadon, A. Jengo, D. Schinella, A. Jus, D. Villalta, P. De Paoli, G., Santini, and F. Tesio (1984). *J. Nephrol.* **4**, 280–286.
20. L. J. Elsas and L. E. Rosenberg, (1969). *J. Clin. Invest.* **48**, 1845–1854.
21. P. Baxter, J. Goldhill, P. T. Hardcastle, and C. J. Taylor (1990). *Gut* **31**, 817–820.
22. T. Yamamoto, Y. Seino, H. Fukumoto, G. Koh, H. Yano, N. Inagaki, Y. Yamada, K. Inoue, T. Manabe, and H. Imura (1990). *Biochem. Biophys. Res. Commun.* **170**, 223–230.
23. R. N. Fedorak, M. D. Gershon, and M. Field (1989). *Gastroenterology* **96**, 37–44.
24. H. Yasuda, T. Kurokawa, Y. Fuji, A. Yamashita, and S. Ishibashi (1990). *Biochim. Biophys. Acta* **1021**, 114–118.
25. UK Prospective Diabetes Study Group (1998). *Lancet* **352**, 837–853.
26. R. W. Cattrall (1997) *Chemical Sensors*, Vol. 52, Oxford University Press, Oxford.
27. T. D. James, H. Kawabata, R. Ludwig, K. Murata, and S. Shinkai (1995). *Tetrahedron* **51**, 555–566.
28. T. D. James, K. R. A. S. Sandanayake, and S. Shinkai (1995). *Supramol. Chem.* **6**, 141–157.
29. T. D. James, P. Linnane, and S. Shinkai (1996). *Chem. Commun.* 281–288.
30. K. R. A. S. Sandanayake, T. D. James, and S. Shinkai (1996). *Pure Appl. Chem.* **68**, 1207–1212.
31. N. DiCesare and J. R. Lakowicz (2001). *Anal. Biochem.* **294**, 154–160.
32. J. P. Lorand and J. O. Edwards (1959). *J. Org. Chem.* **24**, 769–774.
33. J. H. Hartley and T. D. James (1999). *Tetrahedr. Lett.* **40**, 2597–2600.
34. T. D. James, K. Sandanayake, and S. Shinkai (1994). *J. Chem. Soc. Chem. Commun.* 477–478.
35. T. D. James, K. R. A. S. Sandanayake, R. Iguchi, and S. Shinkai (1995). *J. Am. Chem. Soc.* **117**, 8982–8987.
36. T. D. James, K. Sandanayake, and S. Shinkai (1994). *Angew. Chem., Int. Ed. Engl.* **33**, 2207–2209.
37. C. R. Cooper and T. D. James (1997). *Chem. Commun.* 1419–1420.
38. S. Arimori, M. L. Bell, C. S. Oh, K. A. Frimat, and T. D. James (2001). *Chem. Commun.* 1836–1837.
39. S. Arimori, M. L. Bell, C. S. Oh, K. A. Frimat, and T. D. James (2002) *J. Chem. Soc. Perkin Trans. 1* 803–808.
40. D. D. Perrin and B. Dempsey (1974). *Buffers for pH and Metal Ion Control*, Chapman & Hall, London.
41. J. C. Norrild and H. Eggert (1995). *J. Am. Chem. Soc.* **117**, 1479–1484.
42. J. C. Norrild and H. Eggert (1996). *J. Chem. Soc., Perkin Trans. 2* 2583–2588.
43. M. Bielecki, H. Eggert, and J. C. Norrild (1999). *J. Chem. Soc., Perkin Trans. 2* 449–455.
44. G. Lecollinet, A. P. Dominey, T. Velasco, and A. P. Davis (2002). *Angew. Chem. Int. Ed. Engl.* **41**, 4093–4096.
45. K. Sandanayake, K. Nakashima, and S. Shinkai (1994). *J. Chem. Soc., Chem. Commun.* 1621–1622.
46. H. Kijima, M. Takeuchi, and S. Shinkai (1998). *Chem. Lett.* 781–782.
47. A. S. Droz, U. Neidlein, S. Anderson, P. Seiler, and F. Diederich (2001). *Helv. Chem. Acta* **84**, 2243–2289.
48. A. Sugasaki, K. Sugiyasu, M. Ikeda, M. Takeuchi, and S. Shinkai (2001). *J. Am. Chem. Soc.* **123**, 10239–10244.
49. A. Sugasaki, M. Ikeda, M. Takeuchi, and S. Shinkai (2000). *Angew. Chem. Int. Ed.* **39**, 3839–3842.
50. M. Yamamoto, M. Takeuchi, and S. Shinkai (2002). *Tetrahedron* **58**, 7251–7258.
51. M. Ikeda, S. Shinkai, and A. Osuka (2000). *Chem. Commun.* 1047–1048.
52. W. Yang, S. Gao, X. Gao, V. V. R. Karnati, W. Ni, B. Wang, W. B. Hooks, J. Carson, and B. Weston (2002). *Bioorg. Med. Chem. Lett.* **12**, 2175–2177.
53. S. Patterson, B. D. Smith, and R. E. Taylor (1998). *Tetrahedr. Lett.* **39**, 3111–3114.
54. T. Nagase, E. Nakata, S. Shinkai, and I. Hamachi (2003). *Chem. Eur. J.* **9**, 3660–3669.
55. I. Ikeda, S. Shinkai, and A. Osuka (2000). *Chem. Commun.* 1047–1048.
56. S. Arimori, M. D. Phillips, and T. D. James (2004) *Tetrahedr. Lett.* **45**, 1539–1547.
57. C. R. Cooper and T. D. James (1998). *Chem. Lett.* 883–884.
58. P. Collins and R. Ferrier (1995). *Monosaccharides: Their Chemistry and Their Roles in Natural Products*, Wiley, Chichester.
59. S. Arimori, G. A. Consiglio, M. D. Phillips, and T. D. James (2003). *Tetrahedr. Lett.* **44**, 4789–4792.
60. K. Sandanayake, T. D. James, and S. Shinkai (1995). *Chem. Lett.* 503–504.
61. J. R. Lakowicz (1999). *Principles of Fluorescence Spectroscopy*, Plenum, New York.
62. S. Arimori, M. L. Bell, C. S. Oh, and T. D. James (2002). *Org. Lett.* **4**, 4249–4251.
63. T. Jin (1999). *Chem. Commun.* 2491–2492.